diffusion-fundamentals

The Open-Access Journal for the Basic Principles of Diffusion Theory, Experiment and Application

NMR Imaging as a Tool for Studying the Diffusion and Co-Diffusion of Gases in Zeolite Catalysts

J. Fraissard

Université, P. et M. Curie and ESPCI, Laboratoire de Physique Quantique
10 rue Vauquelin, 75231 Paris cedex 05, France

ABSTRACT

^{1}H NMR imaging is a powerful technique for studying the diffusion of pure hydrocarbons (for example benzene and n-hexane) during their adsorption in or desorption from a fixed bed of zeolite crystallites. This technique is used to visualize the progression of the diffusing molecules in the zeolite bed and to determine their intracrystallite diffusion coefficients. More importantly, NMR imaging is today the only technique able to give the time dependence of the distribution of two gases during their competitive diffusion.

1- INTRODUCTION

NMR imaging (MRI) techniques were developed in the 70s mainly in the medical and biological fields, using essentially the ^{1}H nucleus but also ^{3}He, ^{19}F ,^{31}P, and more recently hyperpolarized ^{129}Xe nuclei, etc. They can be defined as those which involve at least one spatial coordinate.

The fact that this technique is non-invasive and non-radiative, coupled with the development of more and more powerful equipment and increasingly sophisticated numerical treatment of images, has tended to generalize MRI in the medical field. However, medicine is not the only field of application of MRI, and the 90s saw considerable progress in this technique for the study of porous media. Unfortunately its relatively low spatial resolution makes it impossible to use it for studying microporous and even mesoporous materials at the length scale of the pore size. The best resolution achieved so far is of the order of a few microns. At present the one micron "barrier" appears to be an ultimate limit. Several factors contribute to this: sensitivity problems, diffusional displacement of the spins during measurements, fast nuclear spin relaxation of adsorbed species, the presence of paramagnetic impurities (especially with industrial samples), etc. Despite these difficulties MRI has been successfully used to study solvent penetration and the dynamics of water in polymers [1,2], the structure and dynamics of polymer gels [3], the segregation of grains in blends [4], the permeation resistance of cement [5], pore size distribution mapping [6] as well as the drying kinetics of gels [7]. It can be also used in microporous systems to investigate the diffusion and molecular mobility of water in 4A zeolites [8] or hydrocarbon diffusion in deactivated Y zeolites [9]. In the field of heterogeneous catalysis, MRI is useful for studying the diffusion of a gas through a permeable solid, in particular through a catalytic bed consisting of zeolites. It is performed not only to determine the diffusion coefficient of a gas, out of adsorption

equilibrium, which can be done with other techniques, but also to determine the temporal evolution of the distribution of this gas in the bed. Finally and above all, to the best of our knowledge it is the only technique which at present can be used to determine the evolution of the distribution in the solid of several gases diffusing competitively. This last point is particularly important in heterogeneous catalysis, since the rate of reaction between two reactants is generally proportional to the concentration of each one at each point in the catalytic bed.

We present here an application of this technique to the study of the diffusion of pure or mixed hydrocarbons (benzene, n-hexane) in a fixed bed of HZSM-5 zeolite during their adsorption at room temperature [10]. In particular, we show that it is possible to visualize the distribution of several gases adsorbed competitively, even if certain results are still essentially qualitative.

2- PRINCIPLE OF THE TECHNIQUE

Figure 1 illustrates the principle of the technique. Magnetically equivalent spins in a homogeneous magnetic field B_0 (Figure 1-a) will give a single signal at a resonance frequency ω_0, the intensity of which depends only on their number and is independent of their distribution within the sample. However, if a field gradient, g, is superimposed on B_0 in the z direction the effective field applied to the spins is of the form $B_z = B_0 + g_z$ (Figure 1-b); the resonance frequency and the signal intensity depend then on the position and the density, respectively, of the spins at each point z of the sample. More generally, the application of pulsed field gradients during the NMR pulse sequence used for the detection of the resonance signal leads to concentration profiles of resonating spins in the direction(s) of the gradient(s). It is therefore possible to obtain images in one, two or three dimensions. It should be noted that the signal detected depends not only on the spin density, ρ, at each point of the sample but also on the pulse sequence used, on relaxation, etc. For example, two sequences can be used.

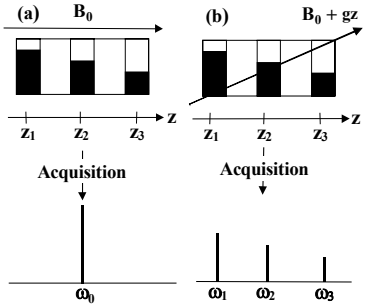

Fig. 1. Principle of 1D NMR Imaging

In the sequence shown in Figure 2-a, the field gradient is applied during the $\pi/2$ pulse and throughout the signal acquisition time, which makes it possible to avoid the problem of spin relaxation and to obtain the real spin concentration profile. In spin echo detection the intensity of the signal depends on relaxation. Figure 2-b details, in this case, the periods during which the gradient is applied depending on the pulses used. This sequence can be

useful when there is a distribution of the spin relaxation times T_2 in the sample, as has been shown in a study of Y zeolite deactivation during catalytic cracking [9].

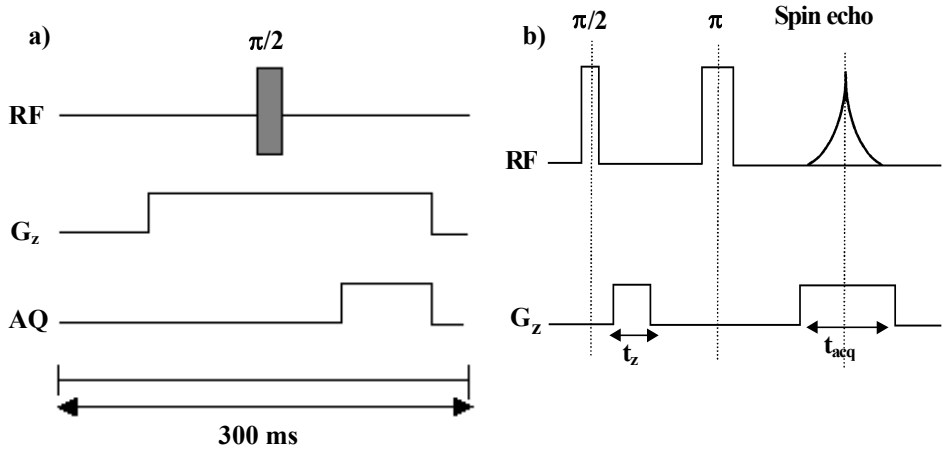

Fig. 2. Schematic representation of the 1D Imaging NMR sequence:
a) Direct acquisition;
b) Spin echo acquisition.

3- EXPERIMENTAL SECTION

HZSM-5 zeolite consisting of crystallites, assumed to be spherical, of average radius R = 20 μm, was used in the form of a powder or compressed (at 10^3 bar) into cylindrical pellets 7 mm in diameter and between 12 and 25 mm long, either pure or with a binder (amorphous silica-alumina, $S_{BET} \approx 700$ m^2 g^{-1}, mean pore diameter 5 nm). Samples placed in the cell were held under vacuum (10^{-5} mbar) at 673 K overnight before the adsorption of gaseous hydrocarbon(s) at constant pressure at 293 K.

At time t = 0 the sample is put into contact with the supply of liquid hydrocarbon (n-hexane or benzene) in equilibrium with the gas and is then placed quickly in the magnet. The liquid phase is either pure or consists of a mixture such that the two partial pressures of the gases are equal to 60 mbar (assuming that the mixture obeys Raoult's law). To distinguish the hydrocarbons when they are mixed, one is perhydro and the other perdeutero.

The proton 1D NMR images, which represent the concentration profiles of the hydrocarbons along the NMR tube axis, are recorded as a function of time with a Bruker MSL 300 spectrometer. They are obtained by applying a magnetic field gradient ($G_Z \approx 4$ T m^{-1}) along the direction of the NMR tube axis during which a π/2 r.f. pulse (RF) is applied and signal acquisition (AQ) is performed (Figure 1-a). The length of the sample is small enough to permit the application of the excitation pulse during the magnetic gradient.

4- MODEL OF DIFFUSION

The diffusion equations are given by the hydrocarbon mass balance in macropores (eq. 1) and in micropores (eq. 2) [11,12]:

$$\varepsilon_{\text{int}\,er}\frac{\partial c}{\partial t} = D_{\text{int}\,er}\,\varepsilon_{\text{int}\,er}\,\frac{\partial^2 c}{\partial z^2} - 3\left(1-\varepsilon_{\text{int}\,er}\right)\frac{D_{\text{int}\,ra}}{R}\left(\frac{\partial q}{\partial r}\right)_{r=R} \qquad (1)$$

$$\frac{\partial q}{\partial t} = D_{\text{int}\,ra}\left(\frac{\partial^2 q}{\partial r^2} + \frac{2}{r}\frac{\partial q}{\partial r}\right) \qquad (2)$$

where c and q are the hydrocarbon concentrations in macropores and micropores, respectively; z (linear) and r (radial) coordinates in the bed (from the bottom) and in the crystallite (from the centre); D_{inter} and D_{intra} the inter- and intracrystallite diffusion coefficients and ε_{inter} the macroporosity of the sample.

These experiments were conducted at pressures where intercrystallite diffusion is very rapid with respect to intracrystallite diffusion. One can check these conditions from the rectangular concentration profile of the images obtained generally after a short time. In this case only equation 2 is used, with the following initial and boundary conditions:

$$q(r,\, t=0) = 0 \qquad q(r=R,\, t) = q^*(t) \qquad \frac{\partial q(r=0,t)}{\partial r} = 0$$

where q^* is the hydrocarbon concentration at the external surface of crystallite.

The time necesssary to reach equilibrium in the macropores is very short as compared with that necessary to reach equilibrium in the micropores. Consequently, more or less quickly after the beginning of the experiment, the hydrocarbon concentration in the macropores is roughly uniform.

$$c(z\,,\, t) \approx c(l\,,\, t) \approx c_0$$

In this case:

$$q(r=R,\, t) = q^*(t) = q_\infty\,[1\text{-}\exp(\text{-}kt)]$$

where $q_\infty = bc_0\, q_{sa\,t} / (1+ bc_0)$ $\quad k = k_a\, c_0$ $\quad b = k_a / k_b$

q_{sat} is the concentration at adsorption saturation ; k_a and k_b are the adsorption and desorption rate constants, respectively.

This kind of diffusion has been solved by Crank [13]:

$$\frac{M_t}{M_\infty} = 1 - \frac{3D_{intra}}{kR^2}\exp(-kt)\left[1 - \sqrt{\frac{kR^2}{D_{intra}}}\cot\sqrt{\frac{kR^2}{D_{intra}}}\right] + \frac{6kR^2}{\pi^2 D_{intra}}\sum_{n=1}^{\infty}\frac{\exp(-D_{intra}n^2\pi^2 t/R^2)}{n^2(n^2\pi^2 - kR^2/D_{intra})} \quad (3)$$

M_t is the total amount of adsorbed gas at time t and M_∞ the corresponding value at the equilibrium state.

It should be pointed out first of all that the hydrocarbon concentration in the gas phase and in the macropores is always negligible compared to that in the micropores (even right at the beginning of adsorption). Consequently, the integral of the NMR signal observed is proportional to the amount of hydrocarbon in the micropores.

5 – ADSORPTION OF PURE GAS

5 -1: Adsorption of Benzene

At the very beginning of adsorption, ($0 < t < 0.1$ h) the 1D images of benzene adsorbing in the powder HZSM-5 bed show a strong concentration gradient decreasing from the top to the bottom of the sample (length:25 mmm, Figure 3a). When t > 0.2 h rectangular profiles are obtained for the loose as well as for the compressed powder (length:12 mm, Figure 3b) proving that after this time, under these experimental conditions (high pressure of the gas phase) the benzene concentration is the same in any part of the bed and that the diffusion of hydrocarbon is then controlled by the micropores, as discussed by Heink et al. [14]. Since compressing the powder increases the density of the sample, the NMR signal is better defined for the compressed sample. This experiment allows the determination of D_{intra}. The signal intensity increases with the adsorption time. The experimental kinetic curves of $M(t) = f(t)$ are simulated using equation 3. The simulation gives a D_{intra} value of about 1×10^{-14} m^2 s^{-1} whatever the form, powder or pellet, of the sample. This value agrees well with that obtained by ^{129}Xe NMR [15]. On the contrary, two different values of k are obtained: 1.2 10^{-3} and 0.8 10^{-3} s^{-1} for the loose and the compressed powder, respectively. The rate of adsorption at the external surface decreases with the size of the intercrystallite space due to the compression of the sample.

When the sample is the powder zeolite mixed with silica-alumina (60% weight of zeolite, length 25 mm), the benzene concentration profiles (Figure 4-a) present an adsorption front which lasts more than 30 min. On one hand, the intercrystallite diffusion rate is decreased by the presence of the mesoporous silica-alumina; on the other hand benzene also adsorbs on the silica-alumina. In the case of a compressed mixed sample (length 12 mm) the profiles are rectangular as of the first spectrum (Figure 4-b). The difference between the two cases is due partly to the decrease in the macroporosity but mainly to the length of the sample. These results show that mass transport in industrial catalysts depends greatly on the binder, the dimensions and the compression of the sample.

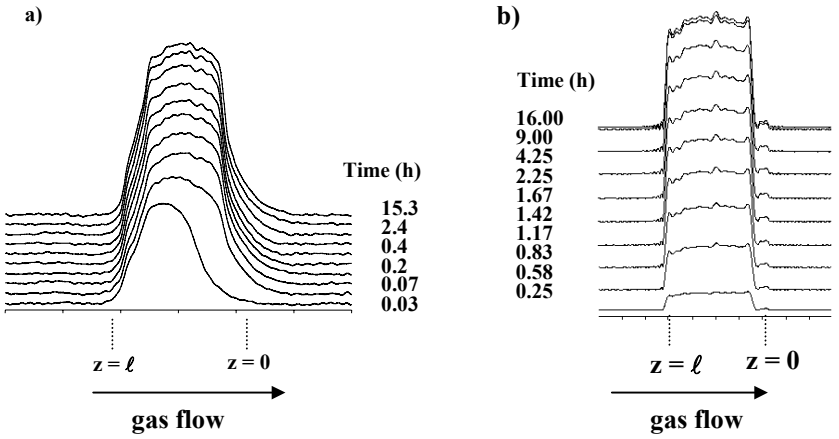

Fig. 3. 1D-NMR profiles of adsorbed benzene: a) on powder (length:25 mm), b) on pellet (length: 12 mm)

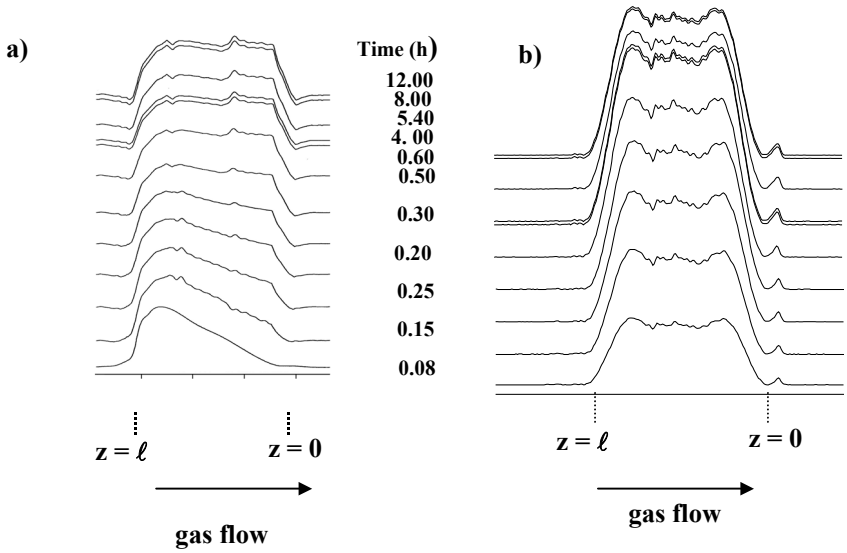

Fig. 4. 1D-NMR profiles in a mixture (zeolite/silica-alumina binder) during benzene adsorption: a) powder (length: 25 mm), b) pellet (length: 12 mm).

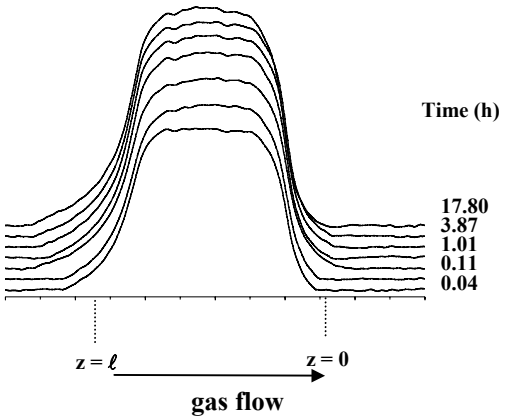

Fig. 5.1D-NMR profiles of n-hexane adsorbed in HZSM5 zeolite in powder form.

5 - 2: Adsorption of hexane

In the case of n-hexane adsorption on a loose powder sample, the concentration profiles (Figure 5) become perfectly rectangular after only t = 0.03 h. The value obtained for D_{intra} ($\approx 10^{-13}$ m^2 s^{-1}) is of the same order of magnitude as that reported in the literature using other techniques (zero length column, frequency response, etc.).

6-DIFFUSION OF GAS MIXTURES

Different types of experiments were performed with n-hexane and benzene. Here we report the results concerning: *i*) their competitive adsorption, *ii*) the variation of the distribution of a pre-adsorbed hydrocarbon during the adsorption of a second one.

6 -1. Competitive adsorption.

When the adsorption of n-hexane proceeds from a gas phase mixture of n-hexane C_6H_{14} and deuterated benzene C_6D_6, both at the same partial pressure, 60 mbar, the intensity of the profiles first decreases from the top to the bottom of the bed (Figure 6-a). Such a profile, which indicates an hexane concentration gradient in the sample, persists up to a time of 0.13 h, whereas the adsorption of pure hexane leads very rapidly to rectangular profiles (Figure 5).

At intermediate time, there is a slight excess of n-hexane in the bottom of the bed before a homogeneous distribution all over the bed is reached at equilibrium. The benzene molecules, whose intracrystallite diffusion is slower than that of n-hexane, progress along the bed and adsorb then on the subsequent layers whose crystallites are free of any adsorbate. As time increases, benzene also adsorbs on the first layers, displacing n-hexane towards the bottom where n-hexane displaces in turn the benzene molecules to finally obtain a distribution governed by thermodynamics. This scenario is confirmed by the evolution of the benzene concentration along the bed, recorded during an identical experiment in which benzene C_6H_6 and deuterated n-hexane C_6D_{14} were used (Figure 6-b).

These two complementary experiments can be explained as follows. The intracrystallite diffusion of hexane is ten times faster than that of benzene, so hexane molecules are faster adsorbed by the very first layers of ZSM-5 crystallites. These partly

reject the benzene molecules which are then at first primarily adsorbed at the end of the column (which n-hexane has not yet reached).

However, this distribution of the molecules must be nuanced. In fact, under the same experimental conditions the signal of hexane, which has 14 hydrogen atoms, is more than twice as strong as that of benzene, which only has 6. Direct comparison of the molecule concentrations in figures 6-a and 6-b requires therefore that the intensities of the hexane signals be divided by a factor of 2.3.

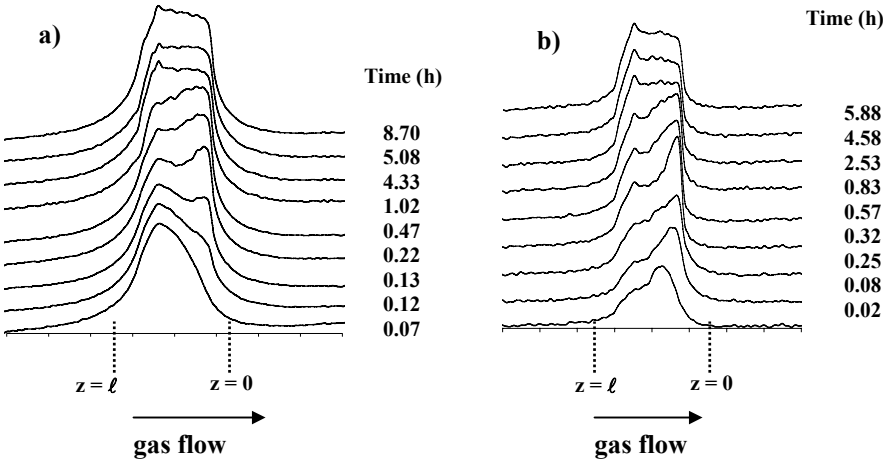

Fig. 6. 1D-NMR profiles of n-hexane a) and benzene b) during their competitive adsorption in HZSM-5 zeolite.

The intermediate states of the systems are the result of competing kinetic and thermodynamic effects, the diffusion of n-hexane being faster than that of benzene while the latter is more strongly adsorbed inside the crystallite.

6 -2. Distribution of pre-adsorbate during the adsorption of another gas

Figure 7 shows the evolution of the distribution of n-hexane C_6H_{14} pre-adsorbed at 2 mbar during the adsorption of deuterated benzene C_6D_6 at its saturation vapour pressure. During C_6D_6 adsorption, the sample stays also under the previous partial hexane pressure. At time $t = 0$, the concentration profile of pre- adsorbed n-hexane is quasi-rectangular. Immediately upon contact with benzene, hexane desorbs from the upper layers of the bed. However, a practically rectangular concentration profile is obtained rapidly, in about 0.2 h. It should be noted that the amount of hexane desorbed between the beginning of the experiment and the attainment of a new equilibrium is about 40%.

Figure 8 corresponds to the case of benzene C_6H_6 being pre-adsorbed at equilibrium at 6.4 mbar and n-hexane C_6D_{14} adsorbing at its saturation pressure. In this case also, during the C_6D_{14} adsorption, the sample stays under the previous partial benzene pressure. We initially observe a rectangular profile corresponding to a uniform distribution of benzene. The total signal area decreases slowly with time. The decrease in the benzene concentration between the beginning and the end of the experiment is about 25 %.

However, its distribution in the sample is particularly inhomogeneous. The intensity decreases at the top and increases markedly at the bottom of the bed, showing that the n-hexane adsorbs first in the upper layers, "pushing" the benzene towards the bottom of the tube. The local partial pressure of benzene and, in parallel, its concentration in the bottom of the bed increase.

As the "wave" of n-hexane reaches the bottom, this latter gas adsorbs on the lower layers; the two partial pressures become uniform along the sample, and the benzene molecules can adsorb again in the upper layers until the thermodynamic equilibrium is obtained. The distribution of adsorbed gases is first determined by kinetics and then the system is governed by thermodynamics.

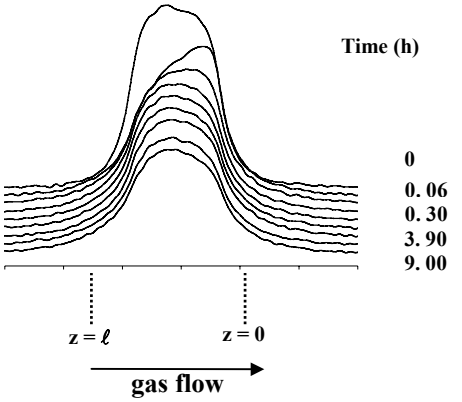

Fig.7: 1D-NMR profiles of pre-adsorbed C_6H_{14} during C_6D_6 adsorption in HZSM-5.

The difference in the extent of displacement of one gas by another in the two experiments confirms, if this were necessary, the greater affinity of HZSM-5 zeolite for benzene.

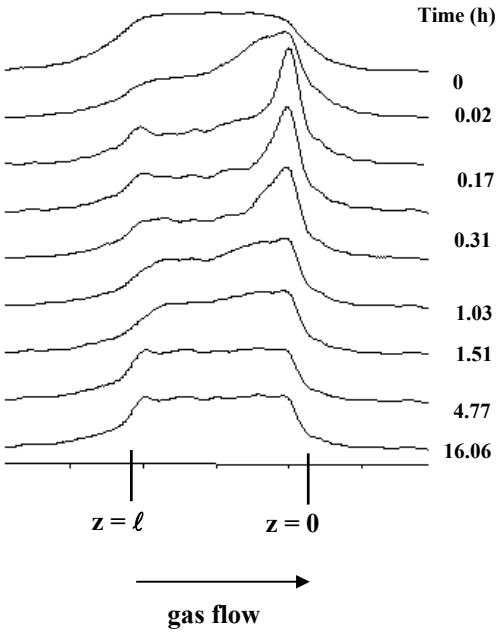

Fig.8: 1D-NMR profiles of pre-adsorbed C_6H_6 during C_6D_{14} adsorption in HZSM-5.

7. CONCLUSION

The application of ^1H 1D-MRI for the study of hydrocarbon diffusion gives two types of information. First, the variation with time of the area of the full signal (amount adsorbed as a function of time) during adsorption makes it possible to determine transport coefficients by simulation of the kinetic curves. For example, the intracrystallite diffusion coefficients of hexane and benzene in HZSM-5 determined by this technique are 10^{-13} and 10^{-14} m^2 s^{-1}, respectively, in good agreement with data in the literature. Second, the shape of the instantaneous concentration profiles reflects the variation of the local adsorbate concentration, and reveals a competition between kinetic and thermodynamic effects.

In the case of competitive adsorption of several gases, this technique appears to be the only one capable of visualizing the relative distribution of each of the gases in the adsorbate and its variation with time.

REFERENCES

1. S. Blackband and P. Mansfield, J. Phys. C: Solid State Phys., 19 (1986) L49.
2. N. Tanaka, S. Matsukawa, H. Kurosu and I. Ando, Polymer, 39 (20) (1998) 4703.
3. I. Ando, H. Kurosu, S. Matsukawa, A. Yamasaki, A. Hotta and N. Tanaka, Wileys Polym. Networks Group Rev., Ser. I (1998) 331. J. Wiley & Sons, Ltd. Publ.
4. P. Porion, N. Sommier and P. Evesque, Europhysics-Letters, 50 (3) (2000) 319.
5. G. Papavassiliou, M. Milia, M. Fardis, R. Rumme, E. Laganas, A. Sepe, R. Blinc, M.M. Pintar J. Am. Ceram. Soc., 76 (1993) 2109.
6. J.H. Strange, J.B.W. Webber and S.D. Schmidt, Magnetic Res. Imaging, 7-8 (1996) 803.
7. I. Koptyug, V.B. Fenelonov, MY. Khitrina, R.Z. Sagdeev and V.N. Parmon, J. Phys. Chem., B, 102 (1998) 3090.
8. M.R. Halse, Magnetic Res. Imaging, 7-8 (1996) 745.
9. J.-L.Bonardet, T. Domeniconi, P. N'Gokoli-Kekele, M.-A. Springuel-Huet and J. Fraissard, Langmuir, 15 (1999) 5836.
10. M.-A. Springuel-Huet, J.-L.Bonardet and J. Fraissard, Proceedings 13th International Zeolite Conference. Elsevier Publ. 2001
11. E. Ruckenstein, A.S. Vaidyanathan and G.R. Youngquist, Chem. Eng. Sci., 26 (1971) 147.
12. L.K. Lee, AIChE. J. 24 (1978) 531
13. J. Cranck, The Mathematics of Diffusion, Clarendon Press, U. K. Oxford, 1956.
14. W. Heink, J. Kärger and H. Pfeifer, Chem. Eng. Sci., 33 (1978) 1019.
15. M.-A. Springuel-Huet, P. N'Gokoli-Kekele, P. Mignon, J.-L.Bonardet and J. Fraissard, Stud. Surf.Sci. Catal., 135 (2001) 3121-3128.